PREDICTION OF AERODYNAMIC COEFFICIENTS OF MISSILE USING PANEL METHOD

Prof. Kamil I. AL-Doulaimi College of Miltary
Asst. Prof Hussain Y. M. **Wisam Mohsin Jabur** College of Eng. / University of Baghdad

ABSTRACT
The low order panel method with Neumann boundary condition have been used to predict the normal force curve slope, the pitching moment curve slope, the center of pressure location and the aerodynamic load distribution for missile in compressible, steady flow. The wing-body-canard interference problem have been solved using two schemes (iterative method and internal singularity method) both are based on the panel method. The normal force curve slope, the pitching moment curve slope and the center of pressure location for a given missile has been predicted using the present numerical method and the DATCOM technique.

الخلاصة

تم استخدام طريقة الأواح ذات الدرجة الواطئة مع الظروف المحيطة لنيومان وذلك للتنبا بميل المنحني للقــوة العمودية ، عزم الطول، موقع مركز الضغط وتوزيع الأحمال الايروديناميكية لصاروخ في جريان انضغاطي مستقر، أن مشكلة تداخل الجناح مع الجسم ومع الزعنفة الجانبية تم حلها بواسطة طريقتين (طريقة التكــرار وطريقة الوحدة الداخلية) والطريقتان اساسها طريقة الألواح . أن ميل منحي القوة العمودية ، عزم الطول ، وموقع مركز الغضط للصاروخ المعتمد تم التنبأ به باستخدام الطريقة العددية الحالية وتقنية DATCOM

KEY WORDS
Missile aerodynamic, panel method, wing-body aerodynamic, prediction of aerodynamic coefficients, potential flow simulation.

INTRODUCTION

Preliminary design and aerodynamic assessment of missile configuration require a rapid and accurate method to predict the aerodynamic coefficients. Accurate calculation of flow field around complete missile is essential to provide aerodynamic data for the structural designer, the performance engineer and the designer of the control system. Three different methods can be employed to determine the missile aerodynamics: 1) wind tunnel tests, 2) Handbooks, 3) C.F.D techniques. Current trends in the design of missile emphasize renewed interest of industry in computational methods capable of supporting aerodynamic design. Within existing teehniques in this region, finite difference methods solving either the full potential or Euler's equators have made the most significant advances in recent years. However, the lack of efficient numerical procedures to generate the computational grid around arbitrary three-dimensional configurations is still a major

problem area for these methods. The Panel Method has been demonstrated to be the most efficient approach to the solution of inviscide flows around arbitrarily complex three-dimensional configurations, since it has the distinct advantage over the alternative C.F.D techniques (finite difference, finite element, etc.) in the fact that the unknowns are situated on the surface of the configuration and not throughout the external space. Therefore, the panel method is very attractive for routine use and amenable for use on medium or small computing facilities since it requires much less programming effort and computing time if compared with the other C.F.D techniques.
The purpose of the present work is to predict the normal force curve slope, pitching moment curve slope and the center of pressure location for a given missile configuration at steady, subsonic and compressible flow using the low order panel method with Numann boundary condition.

PANEL METHOD

The Panel Method is based on distributing singularity elements on the wetted surface of the body around whith the flow characteristics to be found This will reduce the solution to finding the strength of each singularity element that have been distributed.
The incompressible, irrational continuity equation, in terms of the total potential ϕ^* 0 is presented in Ref.[Joseph Katz, 1991] as:

$$\nabla^2\phi^* = 0 \qquad (1)$$

where the total potential 0 is described as ϕ^*

$$\phi^* = \phi + \phi_\infty \qquad (2)$$

Following Green's identity, the general solution to equation (1) can be constructed by sum of sources a and doublets μ:

$$\phi^*_{(x,y,z)} = \frac{1}{4\pi}\int_{body+wake} \mu n.^{\varpi}\nabla(\frac{1}{r})ds - \frac{1}{4\pi}\int_{body} \sigma(\frac{1}{r})ds + \phi_\infty \qquad (3)$$

The Neumann Boundary Condition has been employed with Eq.(3), where a zero normal velocity componen $\partial\phi^* l\partial n = 0$ is directly specified on the surface:

$$\nabla(\phi + \phi_\infty).n^{\varpi} = 0 \qquad (4)$$

Where ϕ^* is the perturbation potential consisting of the two integral terms in Eq.(3). Satisfying this boundary condition in Eq. (3) results in:

$$\frac{1}{4\pi}\int_{body+wake} \mu.^{\varpi}\nabla\left[\frac{\partial}{\partial n}(\frac{1}{r})ds - \frac{1}{4\pi}\int_{body} \sigma\nabla(\frac{1}{r})ds + \nabla\phi_\infty\right].n^{\varpi} = 0 \qquad (5)$$

By knowing the strength of the singularity elements that have been distributed, Eq. (5) will describe the velocity field every where. If we apply this integral equation to each surface panel, and further assume that the singularity strength on each panel is constant, then a system of relatively simple algebraic equations can be obtained in matrix form as:

$$[a_{ij}][k_j] = [-]Q^{\omega}_{\infty}.n^{\varpi}_i \qquad (6)$$

Where k is any singularity element, a_{ij} is the influence coefficient which its physical means The normal velocity induced by a unit strength singularity element at a point in the flow field

[Chun-Mo Lee, 1984]. The only unknown in this matrix equation is the N singularity element strength. The solution of this matrix by Gaussian elimination method results in these unknowns. Any other standard matrix method can be used Since these algebraic equations has a dominated diagonal because the influence of the singularity element on it self is the maximum.

COMPRESSIBILITY EFFECT

The Prundth, JIauert and Gothert rule [Herman Schlichting , 1979] is applied to treat the compressibility effect. This approach is transforming the real body in compressible flow filed to an equivalent body in incompressible flow field by multiplying the Y and Z dimensions of the body and the angle of attack by β:

X_{inc} $\alpha_{\text{inc}} = \beta\alpha$

$Y_{inc} = \beta Y$ $\cot\Lambda_{\text{inc}} = \beta \cot \Lambda$

$Z_{inc} = \beta Z$

Where $\beta = \sqrt{1 - M_{\infty}^{2}}$

After the incompressible flow solution due to this equivalent body is determined, the transmission is reversed to the compressible plane by dividing the resulting aerodynamic coefficients by β^2

NUMERICAL PROCEDURE

Each configuration (wing-body or wing-body-canard) is subdivided into a non-lifting component (body) and lifting components (wing and canard). The non-lifting component is simulated by a constant strength quadrilateral source elements, while the lifting component is simulated by either horseshoe vortex or a vortex ring singularity elements.

THE BODY

The method pioneered by Hess and Smith [Hess, J. L., 1967] forms the basic solution for the body in this work, where the body is replaced by a large number of flat panels, each one carrying a constant strength, quadrilateral source singularity element as in **Fig.(1)**. The body is assumed to be cylindrical with circular cross section and described by number of points on its surface. These points are organized in sections and meridians as shown in **Fig.(l),** short straight lines connecting these points forming quadrilateral panels with the exception of certain regions where the lines converge and the elements are triangular, each panel is a constant strength source singularity element and contains a collocation point placed in the centroid of the panel area.

After obtaining the strength of each source element have been distributed on the body surface the total perturbation velocity components that induced at any collocation point is obtained by summing the perturbation velocities that induced by every source element at this collocation point. The total velocity Q at any collocation point is obtained by summing the total perturbation velocity q and the free stream velocity Q_{∞} that acting on this panel and by using Bernoulli equation [Joseph Katz, 1991], the pressure coefficient at any panel is optioned as:

$$C_{pi} = \frac{P_i - P\infty}{0.5\rho Q_{\infty}^{2}} = 1 - \frac{Q_i^2}{Q_{\infty}^{2}} \qquad (\text{i} = 1 \text{ to NB}) \qquad (7)$$

where

$$Q_i = q_i + (Q_{\infty})_i \qquad (8)$$

The normal force coefficient, the pitching moment coefficient around the nose apex as shown in **Fig.(2)**, and the center of pressure are calculated as:

$$C_N = \frac{1}{S_{ref}} \sum_{i=1}^{NB} C_{Pi} A_i nz_i \qquad (9)$$

$$C_m = \frac{1}{S_{ref} L_{ref}} \sum_{i=1}^{NB} C_{pi} A_i \left[nx_i . (Z_C)_i + nz_i . (X_C)_i \right] \qquad (10)$$

$$\frac{X_{CP}}{L_{ref}} = -\frac{C_m}{C_N} \qquad (11)$$

THE WING AND THE CANARD

The wing and the canard are must be uncambered with zero thickness and simulated by distributing either horseshoe vortices or vortex rings on the surface. The main advantage of these singularity elements is in the simple programming effort required, in addition, they are capable of modeling the effect of wing planform shapes on the fluid dynamic load [Joseph Katz, 1991]. For wingbody configurations, the wing is simulated by distributing horseshoe vortices on the wing surface. While for wing-body-canard configurations, the lifting components (wing and canard) are simulated by distributing a vortex ring singularity elements, since the wake shape for this type of elements can be modeled, where this property is required to simulate the effect of the canard's wake on the wing behind.

HORSESHOE VORTEX

The wing planform is defined by the span, leading edge and trailing edge sweep angles, and divided into NW trapezoidal flat panels with side edges parallel to the global X-axes as shown in **Fig.(3).** Each panel is defined by the coordinates of it's four corners points, and approximated by a flat plate contain a horseshoe vortex. A typical horseshoe vortex element is shown in **Fig.(4)** where the bound vortex is placed at the panel quarter chord line and the collocation point at the center of the panel's , , three-quarter-chord line. The trailing vortices are placed parallel to the global X-axes. The vortex strestr is assumed to be constant for the horseshoe element and a positive circulation is defined as shown in **Fig.(4)**. The lift on each panel containing a horseshoe vortex element is obtained by using the Kutta-Jaukowski theorem [Jack Moran, 1984]:

$$L_i = \rho \nabla y_i Q_\infty \Gamma_i \qquad (\text{i} = 1 \text{ to NW}) \qquad (12)$$

Where ∇y_i is the span of each wing panel. The overall wing lift coefficient, moment coefficient around the wing root cord apex and the center of pressure location are:

$$C_L = \frac{1}{0.5 Q\infty S_w} \sum_{i=1}^{NW} \nabla y_i \Gamma_i \qquad (13)$$

$$C_m = \frac{1}{0.5 Q\infty S_w Cr} \sum_{i=1}^{NW} \nabla y_i \Gamma_i . (X_C)_i \qquad (14)$$

$$\frac{X_{C.P}}{Cr} = \frac{C_m}{C_L} \qquad (15)$$

Where $(XC)_i$ is the global X-coordinate of the center point of panel i.

VORTEX RING

As have been stated before, this singularity element has been employed with the wing-body-canard configurations. The canard planform is divided into NC trapezoidal flat panels in the same manner that have been employed with the horseshoe vortex singularity element, each panel contains a vortex ring singularity element as shown in **Fig.(5).** The leading segment of the vortex ring is placed on the panel's quarter chord line. The collocation point is placed at the center of the Three-quarter

chord line. The normal vector $\overset{\omega}{n}$ is defined at this point and positive circulation is defined as shown in **Fig.(5).**

The canard's wake is aligned in parallel with the free stream and divided into five panels in the stream wise, each wake panel contains a vortex ring with strength equals to the strength of the shading panel at the canard trailing edge as shown in **Fig.(5).** The overall length of the wake is twenty times the span. The wing planform have been divided into NW trapezoidal panels in the same manner that described above, with a deference that the span of each wing panel was made equal to the span of the shading canard panel, as shown in **Fig.(5)**. Also, the wing wake was treated in the same way that has been employed with the canard's wake. The Kutta condition is satisfied along the trailing edge by setting the strength of each wake vortex equal to the strength of the shading panel at the trailing edge, i.e.:

$$\Gamma_W = \Gamma_{T.E} \qquad (16)$$

The lift force that acting on each panel containing a vortex ring singularity element have been calculated by using another form ofKutta-Jaukowski theory [7]:

$$L_{ij} = \rho Q_\infty (\Gamma_{i,j} - \Gamma_{i-1,j}) \nabla y_{ij} \qquad (i > 1) \qquad (17)$$

Where j is a spanwise counter which have values from one to the number of the panels in the spanwise, and i is a cordwise counter which have values from one to the number of the panels in the cordwise as shown in **Fig.(7)**, this figure also shows the sequence of scanning for wing or canard panels to obtain the lift on each panel from Eq.(16). Eq.(16) is applied to the panels that placed after the leading edge panel (i.e. i>l), while for the leading edge panels (i.e. i=l), the lift is calculated as:

$$L_{ij} = \rho Q_\infty (\Gamma_{i,j} \nabla y_{ij} \qquad (i = 1) \qquad (18)$$

The total lift and moment acting on the wing are:

$$C_L = \frac{\sum_{K=1}^{NW} L_{ij}}{0.5 \rho Q_\infty^2 S_w} \qquad (19)$$

$$C_m = \frac{\sum_{K=1}^{NW} L_{ij} . (X_C)_{ij}}{0.5 \rho Q_\infty^2 S_w Cr} \qquad (20)$$

WING-BODY-CANARD INTERFERENCE

The interference between the canard and the body is similar in its physical nature to the wing-body interference. In addition, the influence of the downwash behind the canard on the wing lift has been

taken in account. Three different methods have been employed to describe the wing-body-canard interference:

ITERATIVE METHOD

The following steps can describe it:

1- In the free stream, calculate the strength of each source panel on the fuselage surface.
2- In the flow field interfered by the fuselage, calculate the strength of each vortex panel on the surface of the canard.
3- Using the vortex and source strength, which obtained from the steps (1) and (2), remodel the flow field by superposition and calculate the strength of each vortex on the wing.
4- Using the vortex strength of the canard and the wing, which obtained from step (2) and (3), remodel the flow field by superposition and recalculate the strength of each source panel on the fuselage surface.
5- Re-obtain the steps (2), (3) and (4) four times.

INTERNAL SINGULARITIES METHOD

A schematic view of this method is shown in **Fig.(8).** Vortex panels have been distributed inside the body in the wing-body junction region, and extended from the wing-body junction line to the body longitudinal axes. The strength of each internal panel vortex equals the strength of the neighboring wing root panel vortex. The same treatment is employed for the canard-body interference.

DATCOM SOLUTION

The DATCOM solution [DATCOM , 1972] is employed to solve the interference problem for the wing-body-canard configuration only. The aerodynamic forces acting on each isolated component of the configuration (wing, body and canard) are predicted from the numerical solution of the panel method. Therefore, the final solution that resulting from this technique is not depending solely on the DATCOM. The lift curve slope and the pitching moment curve slope around the center of gravity for a wingbody-canard configuration can be obtained according to this scheme as follows:

$$C_{La} = (C_{La})_e^{'}\left[K_N + K_{W(B)} + K_{B(W)}\right]\frac{S_e^{'}}{S^{'}} + (C_L)_e^{''}\left[K_N + K_{W(B)} + K_{B(W)}\right] \cdot \frac{q^{''}}{q_\infty}\frac{S^{''}}{S^{'}}\frac{S_e^{''}}{S^{''}} + (C_{La})_{W^{''}(V)} \qquad (21)$$

$$C_{ma} = -\frac{X_{c.g} - X^{'}}{\bar{C}^{'}}\left[K_N + K_{B(W)} + K_{W(B)}\right](C_{La})_e^{'}\frac{S_e^{'}}{S^{'}} - \frac{X_{e.g} - X^{''}}{\bar{C}^{''}}\left(\frac{\bar{C}^{''}}{\bar{C}^{'}}\right)\left\{\left[K_{B(W)} + K_{W(B)}\right]^{''}(C_{La})_e^{''}\frac{S_e^{''}}{S^{''}}\frac{S^{''}}{S^{'}}\frac{q^{''}}{q_\infty} + (C_{La})_{W^{*}(V)}\right\} \qquad (22)$$

The parameter $(CL_a)_{W^{*}(V)}$ represents the effect of canard voracity on the wing lift.

OVERALL LOAD CALCULATIONS

Since the strength of the singularity elements that have been distributed on each component (wing, body and canard) are obtained after solving the interference problem by either the iterative method or the internal singularity method, the aerodynamic loads acting on a wing-body-canard or a wingbody configuration can be calculated. For a wing-body-canard configuration, the total velocity Q at any collocation point on the body surface is obtained by summing the total perturbation

velocity components induced by the body source elements, the wing vortex elements and the canard vortex elements with the free stream velocity components in the local coordinates of the panel under consideration. By substituting this velocity in Eq.(6), the pressure coefficient (Cp) at the panel that containing this collocation point is obtained.
The normal force coefficient and the pitching moment coefficient are obtained from:

$$C_N = \frac{1}{0.5\rho Q_\infty^2 S_{ref} L_{ref}} \left[\left[\sum_{k=1}^{NB} 0.5\rho Q_\infty^2 (C_p)_k A_k .nz_k \right]_{body} + \left[\sum_{k=1}^{NW} L_k \right]_{wing} + \left[\sum_{k=1}^{NC} L_k \right]_{canard} \right] \quad (23)$$

$$C_m = \frac{1}{0.5\rho Q_\infty^2 S_{ref} L_{ref}} \left[\left[\sum_{k=1}^{NB} 0.5\rho Q_\infty^2 (C_p)_k A_k .(nx_k .(Z_C)_k + nz_k .(X_C)_k) \right]_{body} + \left[\sum_{k=1}^{NW} L_k .(X_C)_k \right]_{wing} + \left[\sum_{k=1}^{NC} L_k .(X_C)_k \right]_{canard} \right] \quad (24)$$

Where L_k is the lift force acting on the panel k (of the wing or the canard). Since vortex ring singularity elements have been distributed on the wing and canard panels of the wing-body-canard configuration, the lift L_k is obtained in The same manner that have been described in the Eq.(16) and Eq.(17).

RESULTS AND DISCUSSION

Fig.(9) shows the sketch and the dimensions of two different missiles stated in Ref.[3]. The normal force curve slope has been predicted for missile A, while for missiles B, the center of pressure location as a ratio of the wing root cord have been predicted. Good agreement exists between the experimental data and the present numerical solution. **Fig.(10)** illustrates the sketch and paneling of the configuration of.[Joseph Katz, 1991]. The wing is trapezoidal of aspect ratio 3.2 having a leading edge sweep angle of 29.3 . The canard is located in the plane of the wing and consisted of delta and swept rectilinear surfaces respectively. The lift coefficient of canard-wing combination at incompressible flow. based on the wing area for a configuration of delta canard, swept canard and canard off is predicted by using the internal singularity method as shown in **Fig. (11), (12)** and **(13)** respectively. For all these cases, the present numerical results agree well with the experimental data. The results of the internal singularity method for the three cases together are presented in **Fig.(14),** where the configuration with the swept canard has the greatest lift coefficient, while the configuration without canard (canard off) has the smallest lift coefficient.
Fig.(15) shows the dimensions and the paneling of a given missile, which has been named as the "Typical Canard Missile", it consists of an ogive nose with cylinder body, the body is divided into two cylinders, the first has a diameter of 15.2 cm. and the second has a diameter of 11 cm. The canard is trapezoidal with 40 deg. Leading edge sweep angle, the wing is also trapezoidal with 8.6 deg. Leading and trailing edge sweep angle, mounted in the same plane of the canard. The effect of Mach number on the normal force curve slope is presented in **Fig.(16)**, a slight difference can be observed between the result of iterative method and the internal singularity method, while larger difference was noticed between the result of DATCOM solution and the both techniques of the present numerical solutions (the iterative method and the internal singularity method). However, the same trend can be noticed between the results of these three solutions. **Fig.(17)** describe the effect of Mach number on the pitching moment curve slope around the nose. A slight difference can be noticed between the results of the two schemes of the panel method solution, while the results of the

DATCOM solution is greater with the same trend as the result of the panel method. The difference between the results of the panel method and the DATCOM solution is expected, since the DATCOM solution is based on empirical relations and parameters that driven from the slender body theory. **Fig.(18)** illustrates the center of pressure location and it's variation with the Mach number. The results of the both schemes of the panel method are in similar trend as the DATCOM results, where the center of pressure is shifted backward as the Mach number increased.

Fig.(19) presents the effect of increasing the exposed wing semispan on the aerodynamic characteristics of the typical canard missile. It can be noticed that the normal force and the pitching moment curve slope is increased by increasing the wing span, since the wing area and aspect ratio is increased. This may be attributed to the increasing in the lifting force that generated on the wing (since the wing area and aspect ratio is increased). As a result of this, the center of pressure was shifted in backward direction. The nonlinear relationship which can be noticed between the results of **Fig.(19)** and the wing's exposed semispan is expected, since increasing the wing span changes it's aerodynamic characteristics, and this will effects on the wing-body and the wing-canard interference. The effect of the wing longitudinal position (as a distance from the nose apex) is shown in **Fig.(20)**, the wing was shifted in the backward direction. A slight increasing in the normal force curve slope is noticed. This is believed to be due to reducing the canard's downwash strength that acting on the wing. Since the vertical distance between the wing's surface and the canard's wake is increasing by shifting the wing in backward direction, which leads to reducing the canard's downwash strength that acting on the wing. The pitching moment curve slope is also increased and the center of pressure is shifted in backward direction. The effect of decreasing the body maximum diameter on the aerodynamic characteristics of the Typical Canard Missile is presented in **Fig.(21).** Where the normal force curve slope and the pitching moment curve slope are increased by reducing the body maximum diameter. The center of pressure is shifted backward by decreasing the body maximum diameter. This can be attributed the decrement in the nose surface area and the increment in the nose fineness ratio that happens when the body maximum diameter is decreased, also, reducing the body diameter will reduces the body upwash that acting on the canard. As a result of all this, the normal force that generated from the canard and the nose will decreases. The non-linear relationship between the predicted aerodynamic characteristics and the body maximum diameter that can be noticed in **Fig.(21)** is attributed to the non-linear relationship which already exists between the diameter and the cross-sectional area (since the reference area is the body maximum cross-sectional area). Also, change the body maximum diameter effects the canard-body interference, and change the aerodynamic characteristics of the nose (since it's fineness ratio will changed).

CONCLUSIONS

The comparisons with the experimental data tend to the following conclusions:

1- The low order panel method can predict the aerodynamic characteristics and load distribution for the complex three-dimensional configurations in the linearized, steady, subsonic flow with good accuracy.
2- Since the low order panel method have low computing cost associated with less programming effort if compared with the other C.F.D technique, it is flexible and fast.

Depending on the results that describing the effect of some geometry changes on the aerodynamic characteristics of the typical canard missile, the following conclusions are obtained.

1- The center of pressure can be shifted backwards by either increasing the wing span or decreasing the body maximum diameter, or by shifting the wing backwards.
2- Increasing the wing span shifts the center of pressure backwards with a remarkable increase in normal force curve slope. While almost the same change in center of pressure location can be achieved by shifting the wing backwards, with a difference that the increment in normal force

curve slope in this case is small if compared with the increment that was achieved in the normal force curve slope when the wing span was increased.

3- The change in the center of pressure location, which can be accomplished by changing the body maximum diameter, is much less than the change that results from changing wing span or location.

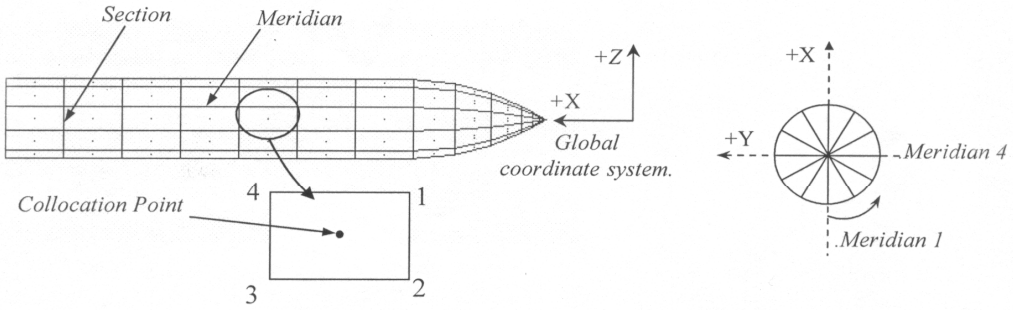

Fig.(1) Body Discretization.

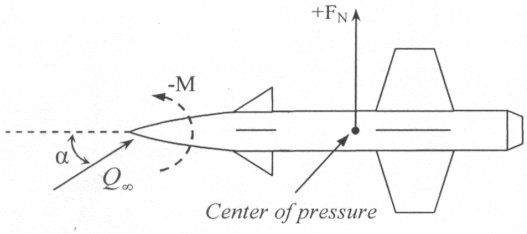

Fig.(2) Normal force and pitching moment around the center of gravity.

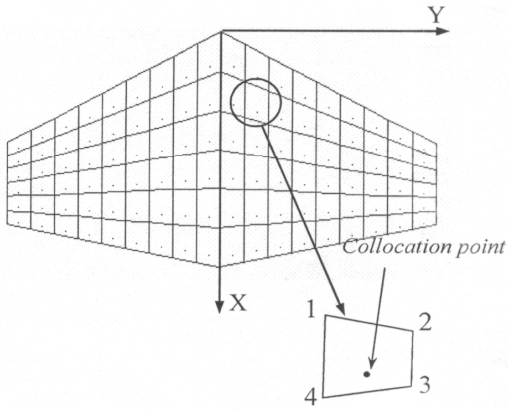

Fig.(3) Wing discretization

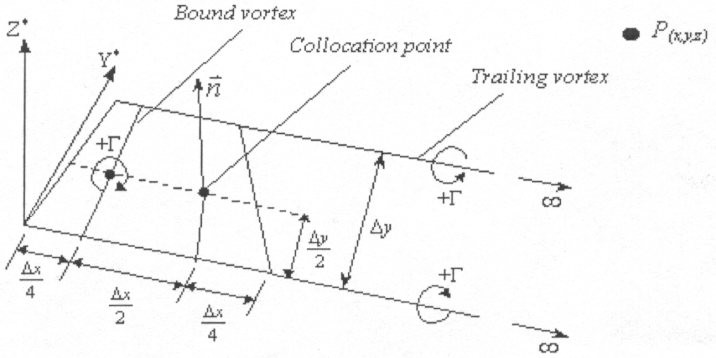

Fig.(4) A typical horseshoe vortex element.

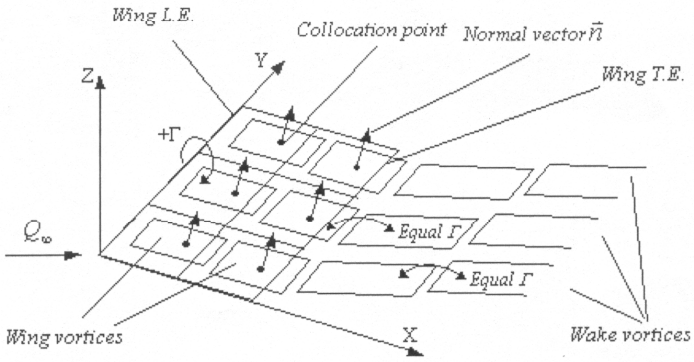

Fig.(5) Vortex ring model for a lifting surface (wing or canard).

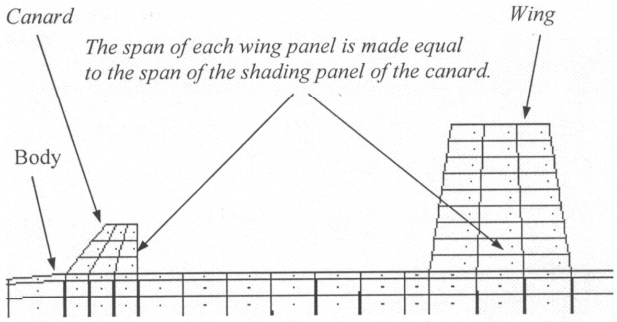

Fig.(6) Wing and canard discretization for wing-body-canard configuration.

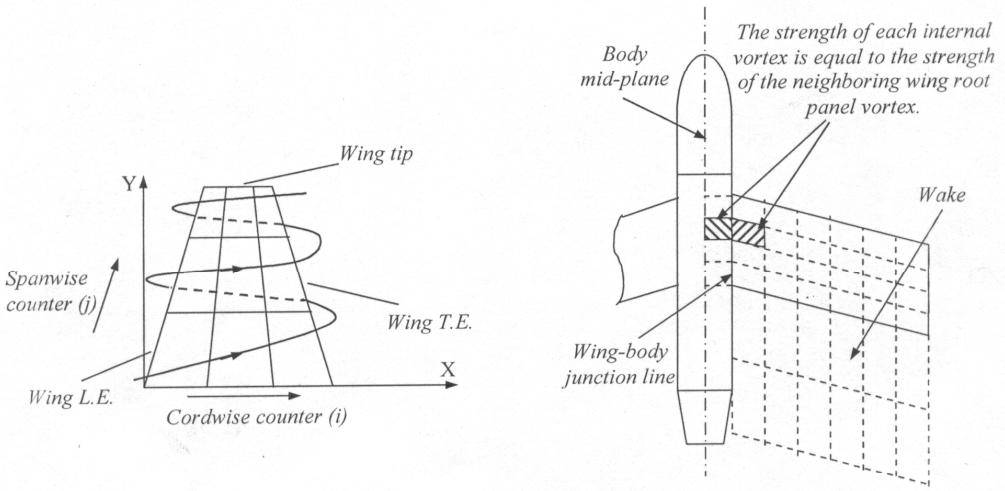

Fig.(7) Sequence of scanning the panels for the wing or the canard.

Fig.(8) Internal Singularities method.

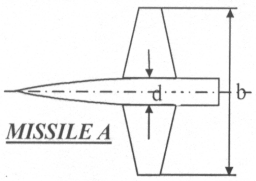

AR=3 AR_e=2.74
λ=0.4 λ_e=0.433
$\Lambda_{L.E}$=19.1° d/b=0.145
$M_\infty = 0.25$ S_e/S=.802

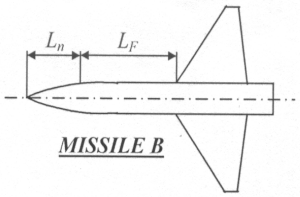

AR=3 AR_e=2.84
λ=0.143 λ_e=0.169
$\Lambda_{L.E}$=38.7° $(C_r)_e$=13.5 in.
d=5 in. b=27.4 in.
L_n=8.75 in. L_F=26.65 in.
$M_\infty = 0.6$ S_e/S=.705

MISSILE A	$C_{N\alpha}$
Experimental result [3]	66.99
Iterative method	68.273
Internal singularity method	67.96

MISSILE B	X_{CP} (inches from the nose apex).
Experimental result [3]	38.909
Iterative method	39.96
Internal singularity method	40.18

Fig.(9) Normal force curve slope and center of pressure position for two different missiles.

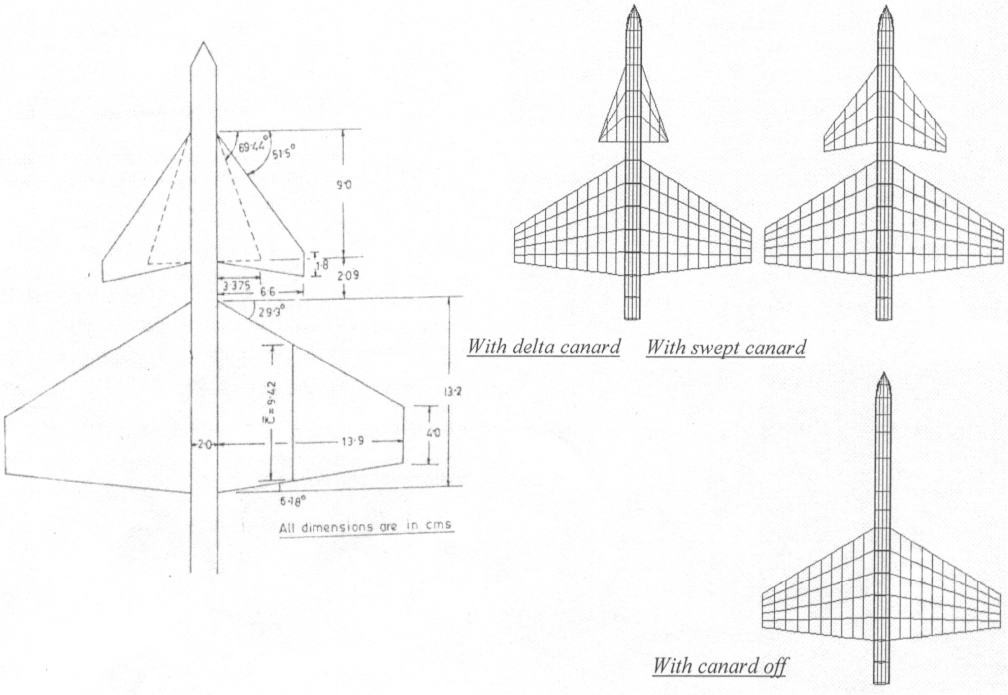

Fig.(10) Sketch and paneling of the configuration of Ref.[1].

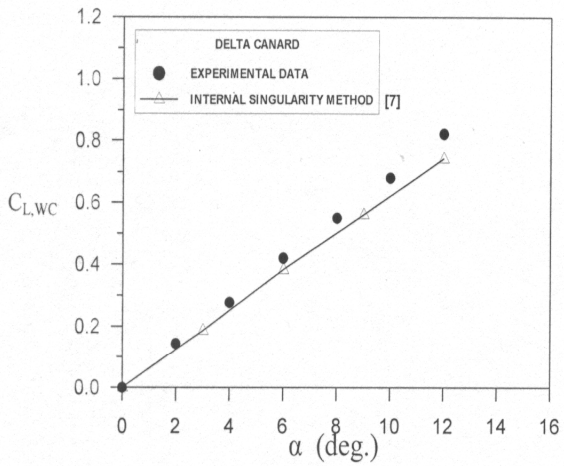

Fig.(11) Variation of lift with incidence for the configuration of Ref.[7] with delta canard.

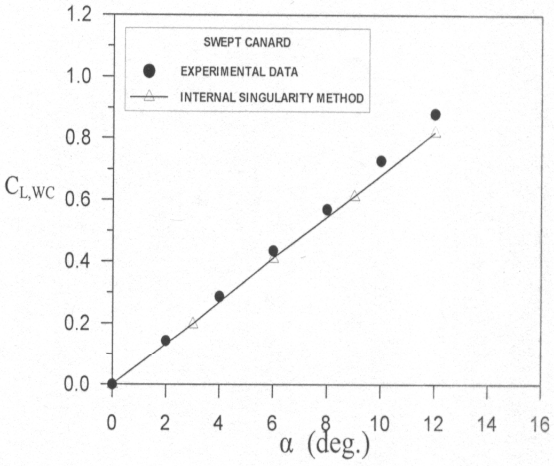

Fig.(12) Variation of lift with incidence for the configuration of Ref.[7] with swept canard.

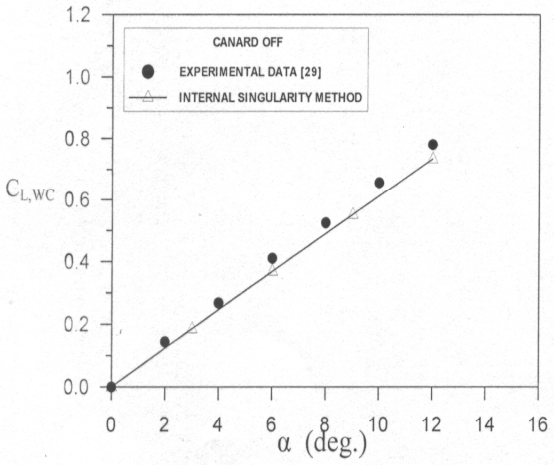

Fig.(13) Variation of lift with incidence for the configuration of Ref.[1] With canard off.

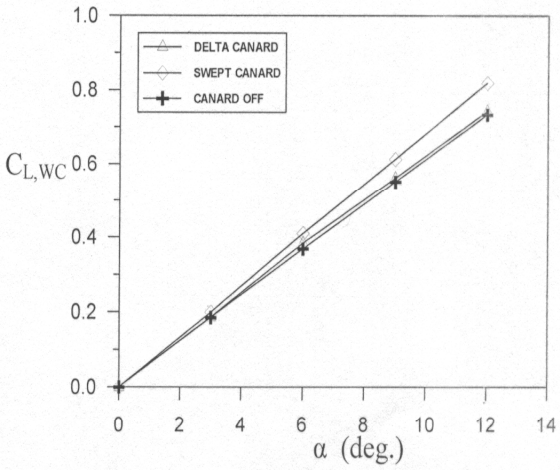

Fig.(14) Variation of lift with incidence for the configuration of Ref.[1].

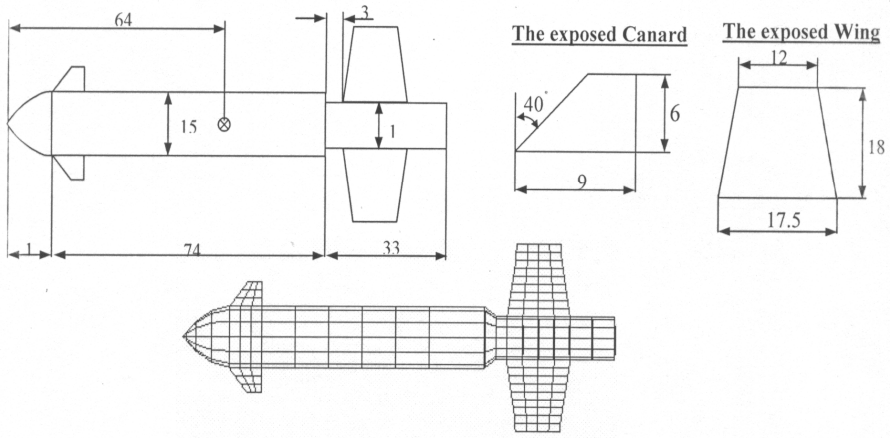

Fig.(15) Sketch and paneling of a typical canard missile,(all dimensions in cm.).

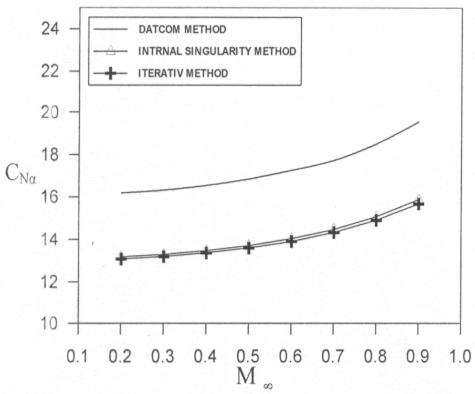

Fig.(16) Mach number effect on normal force curve slope for the Typical Canard Missile.

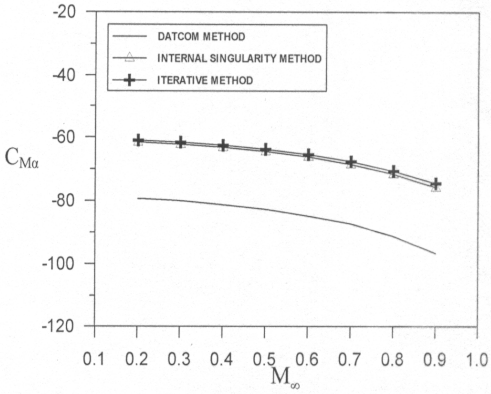

Fig.(17) Mach number effect on pitching moment curve slope for the Typical Canard Missile.

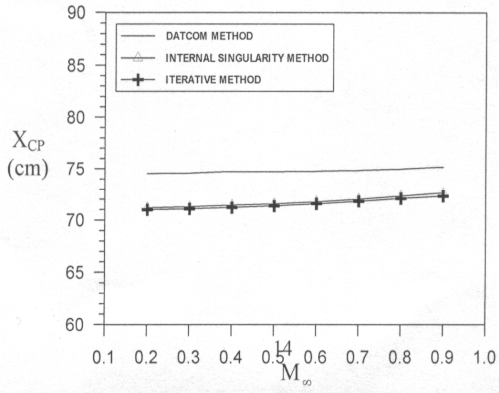

Fig. (18) Mach number effect on center of pressure location for the Typical Canard Missile

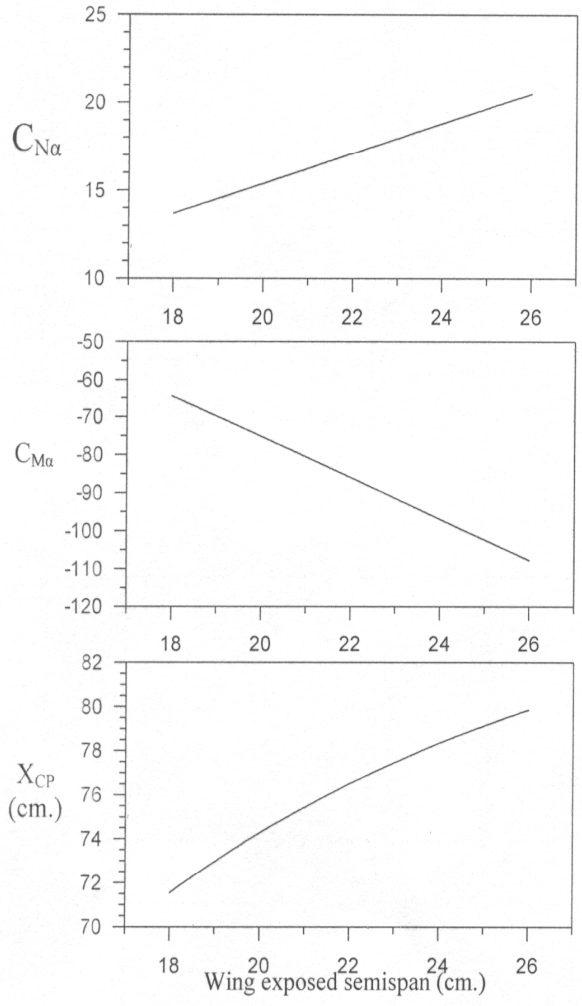

Fig.(19) Effect of increasing wing exposed semispan on the aerodynamic characteristics of the Typical Canard Missile at $M_\infty = 0.5$ using the internal singularity method.

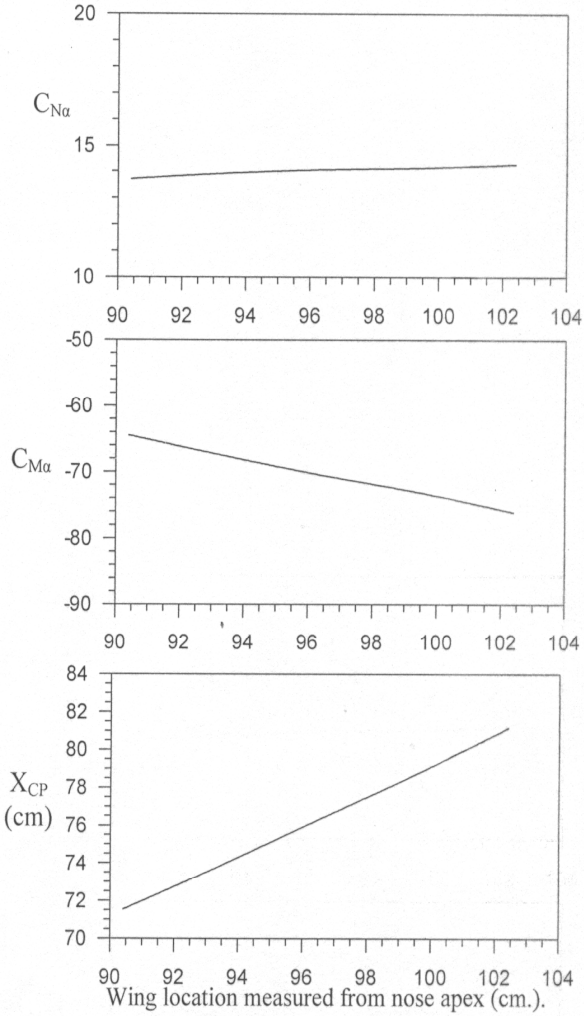

Fig.(20) Effect of wing location on the aerodynamic characteristics of the Typical Canard Missile at $M_\infty = 0.5$ using the internal singularity method.

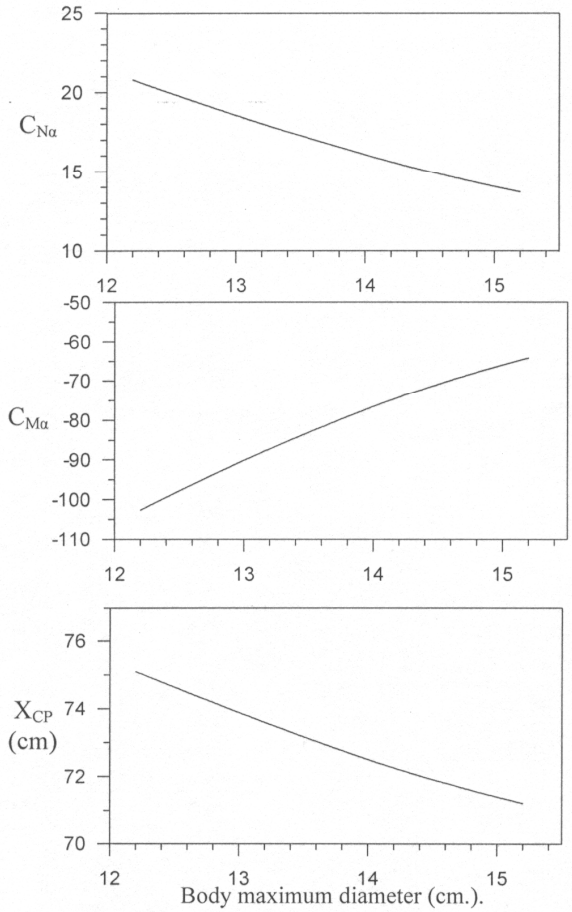

Fig.(21) Effect of body maximum diameter on the normal force, pitching moment curve slope and center of pressure location for the Typical Canard Missile at $M_\infty = 0.5$ using the internal singularity method.

REFERENCES

Bandyopadhyay G., (1989), Low Speed Aerodynamics of Canard Configurations, Aeronautical Journal, January.

Chun-Mo Lee and Sheng-Jil Hsieh, (1984), An Aerodynamic analysis and The Subsequent Motic of External Store, 4th International Conference on Applied Numerical Modeling, Dec. 27- 29Taiwan, R.O.C.

DATCOM, (1972), Douglas Aircraft Co., Inc.,.

Herman Schlichtmgetal (1979), Aerodynamics of the Airplane, McGraw-hill International Boo Company,.

Hess, J. L. and Smith, A. M. O, (1967), Calculation of Potential Flow About Arbitrary Bodies, Progress in Aeronautical Science Journal, Vol. 8, Pergamon Press,

Jack Moran (1984), An Introduction to Theoretical and Computational Aerodynamics, Job] Wiley and Sons,.

Joseph Katz and Alien Plotkin (1991), Low-Speed Aerodynamics, From Wing Theory to Pane Method". McGraw-Hill..

NOMENCLATURI

A	:Panel area
b	:Wing or canard span
$\overline{C}$	:Mean aerodynamic chord
C	:Local wing chord
c.g	:Center of gravity
$C_{L,WC}$	:Coefficient of canard and wing lift, referred to wing area
$C_{L\alpha}$	:Lift curve slope
C_m	:Pitching moment coefficient
$C_{m\alpha}$	:Pitching moment curve slope
C_N	:Normal force coefficient
$C_{N\alpha}$	:Normal force curve slope
Cr	:Wing or canard root chord
C_P	:Pressure coefficient
D	:Body diameter
d''	:Body diameter at the wing-body junction region
d'	:Body diameter at the canard-body junction region
K_N	:Ratio of nose lift
$K_{B(W)}$	:Ratio of body lift in the presence of wing
$K_{W(B)}$	:Ratio of wing lift in the presence of body
L_{ref}	:Reference length (body maximum diameter)
M_∞	:Free stream Mach number
$\vec{n}$	:Unit normal vector
NB	:Number of body panels
$\vec{Q}_\infty$	:Free stream velocity.
$\vec{Q}$	:Total velocity vector .
R	:Radius.
S_w	:Wing or canard planform area.
S_{ref}	:Reference area (body maximum cross-sectional area).
x, y, z	:Global coordinates.
X_c, Y_c, Z_c	:Global coordinates of the panel's center point.
$X_{C.P}$	:Center of pressure location.
$X_{c.g}$	:Center of gravity location.
Δx	:Panel length.
Δy	:Panel span.
α	:Angle of attack.
β	:Mach number prameter $\sqrt{1-M_\infty^2}$.
Γ	:Vortex strength.
$\Gamma_{T.E}$	:Trailing edge vortex strength.
Γ_W	:Wake vortex strength.
θ	:Meridian angle measured from the z-axes.
$\Lambda_{L.E}$	:Leading edge sweep angle.
$\Lambda_{T.E}$	:Trailing edge sweep angle.
ρ	:Air density (1.2 kg/m^3).
σ	:Source strength.
Φ^*	:Total potential.
Φ_∞	:Free stream potential.
Φ	:Perturbation velocity potential.

Superscripts

''	:Related to the wing .
'	:Related to the canard.

Subscripts

NC	:Number of canard panels
NW	:Number of wing panels
P	:Local pressure
P_∞	:Free stream pressure
$\vec{q}$	:Perturbation velocity vector
$\vec{Q}_\infty$	:Free steam velocity vector